

Dynamic equilibrium between cancer stem cells and non-stem cancer cells in human SW620 and MCF-7 cancer cell populations

G Yang¹, Y Quan¹, W Wang¹, Q Fu¹, J Wu¹, T Mei¹, J Li¹, Y Tang¹, C Luo², Q Ouyang², S Chen³, L Wu³, TK Hei^{*,4} and Y Wang^{*,1}

¹State Key Laboratory of Nuclear Physics and Technology, School of Physics, Peking University, Beijing 100871, People's Republic of China; ²Center for Theoretical Biology, School of Physics, Peking University, Beijing 100871, People's Republic of China; ³Key Laboratory of Ion Beam Bioengineering, Chinese Academy of Sciences, Hefei 230031, People's Republic of China; ⁴Center for Radiological Research, Columbia University, VC11-205, 630 West 168th Street, New York, NY 10032, USA

BACKGROUND: Cancer stem cells (CSCs) paradigm suggests that CSCs might have important clinical implications in cancer therapy. Previously, we reported that accumulation efficiency of CSCs is different post low- and high-LET irradiation in 48 h.

METHODS: Cancer stem cells and non-stem cancer cells (NSCCs) were sorted and functionally identified through a variety of assays such as antigen profiles and sphere formation. Inter-conversion between CSCs and NSCCs were *in situ* visualised. Cancer stem cells proportions were assayed over multiple generations under normal and irradiation surroundings. Supplement and inhibition of TGF- β 1, as well as immunofluorescence assay of E-cadherin and Vimentin, were performed.

RESULTS: Surface antigen markers of CSCs and NSCCs exist in an intrinsic homeostasis state with spontaneous and *in situ* visualisable inter-conversions, irrespective of prior radiations. Supplement with TGF- β 1 accelerates the equilibrium, whereas inhibition of TGF- β signalling disturbs the equilibrium and significantly decreases CSC proportion. Epithelial mesenchymal transition (EMT) might be activated during the process.

CONCLUSION: Our results indicate that the intrinsic inter-conversion and dynamic equilibrium between CSCs and NSCCs exist under normal and irradiation surroundings, and TGF- β might have important roles in the equilibrium through activating EMT.

British Journal of Cancer (2012) **106**, 1512–1519. doi:10.1038/bjc.2012.126 www.bjcancer.com

Published online 3 April 2012

© 2012 Cancer Research UK

Keywords: cancer stem cells; inter-conversion; dynamic equilibrium; radiation; epithelial mesenchymal transition

Tissue-specific stem cells exist in many adult tissues and can be identified and isolated using specific antigen profiles. Many, if not all, tumours and established tumour cell lines contain cancer stem cells (CSCs) isolated via cell-surface markers (Dalerba *et al*, 2007; Visvader and Lindeman, 2008). Cancer stem cells are defined by the abilities to self-renew, to differentiate into progeny non-stem cancer cells (NSCCs), and to form tumours effectively upon injection into immunosuppressed mice. These endpoints are commonly complemented by the 'sphere-forming' assay *in vitro* as a useful surrogate (Alison *et al*, 2011). Increasing evidence suggests a central role for CSCs in tumourigenesis, metastasis, radioresistance, as well as tumour recurrence (Bao *et al*, 2006; Diehn *et al*, 2009; Rosen and Jordan, 2009; Alison *et al*, 2011). Importantly, CSC-rich tumours are also associated with aggressive disease and poor prognosis, indicating that an understanding of CSCs biology is pertinent to developing effective therapies (Chaffer *et al*, 2011). In CSC paradigm, CSCs are thought to be self-renewing and to reside at the top of the cellular hierarchy (Dalerba *et al*, 2007;

Clevers, 2011). Through asymmetric division and differentiation, these stem cells generate more differentiated progeny that lack self-renewal capacity. However, recent studies also indicated that CSCs can be spontaneously generated from NSCCs (Meyer *et al*, 2009; Chaffer *et al*, 2011) and more interestingly, can be induced from NSCCs with either chemical treatment (Achuthan *et al*, 2011; Iliopoulos *et al*, 2011) or ionising irradiation (Liang *et al*, 2010). Previously, we also reported that accumulation efficiency of CSCs is quite different post low- and high-LET irradiation in 48 h (Quan *et al*, 2011). The relationships between CSCs and NSCCs have received enormous attention but remain controversial. In addition, the proportion of CSCs remains constant over multiple generations in many established cancer cell lines (Iliopoulos *et al*, 2011), but the basis of this phenomenon is poorly understood.

To address these questions, CSCs and NSCCs from SW620 colon cancer and MCF-7 breast cancer cells were separated through CD133, CD44, and CD24 cell-surface antigen markers, respectively. The results showed that surface antigen markers of CSCs and NSCCs exist in an intrinsic homeostasis state with spontaneous and *in situ* visualisable inter-conversions, irrespective of prior radiations. Supplement with TGF- β 1 accelerates the equilibrium, whereas inhibition of TGF- β signalling disturbs the equilibrium and significantly decreases CSCs proportion. Further, immunofluorescence studies with E-cadherin and Vimentin, markers of epithelial mesen-

*Correspondence: Professor Y Wang; E-mail: ygwang@pku.edu.cn or Professor TK Hei; E-mail: tkh1@columbia.edu
Received 20 January 2012; revised 5 March 2012; accepted 8 March 2012; published online 3 April 2012

chymal transition (EMT), suggested that EMT might be activated during the process. Our results suggest a possible reason for retaining a constant CSC proportion of many established tumour cell lines.

MATERIALS AND METHODS

Cell culture

Human colon cancer SW620 cells and breast cancer MCF-7 cells were purchased from America Type Culture Collection. They were cultured in Dulbecco's modified Eagle's medium supplemented with 10% foetal bovine serum, 100 U ml⁻¹ penicillin, and 100 µg ml⁻¹ streptomycin at 37 °C in 5% CO₂. For some experiments, cells were cultured with or without 0.4 ng ml⁻¹ TGF-β1 (Perprotech, Rocky Hill, NJ, USA) or 1 µM SB431542 (Sigma, St Louis, MO, USA).

Cell staining and flow cytometry

Matched subpopulations were separated as described (Al-Hajj *et al*, 2003; O'Brien *et al*, 2007; Ricci-Vitiani *et al*, 2007). In brief, cells were stained at a concentration of 10⁷ cells per 100 µl of buffer. Anti-CD133/1(AC133)-APC, anti-CD133/1(AC133)-PE (Miltenyi Biotec, Auburn, CA, USA), anti-CD44-PE (BD Pharmingen, San Jose, CA, USA), and anti-CD24-Alex488 (BioLegend, San Diego, CA, USA) antibodies were used for flow cytometric sorting/assay of SW620 and MCF-7 cells, respectively. For all experiments, samples were sorted on a BD FACS Aria II and analysed on a BD LSR II flow cytometer using BD FACS Diva Software (BD Bioscience, San Jose, CA, USA). Side scatter and forward scatter profiles were used to eliminate debris and cell doublets.

Irradiation protocol

Cells were irradiated at room temperature with ⁶⁰Co γ-ray at a dose rate of 1 Gy min⁻¹ for the time required to generate a dose curve of 0, 2, 4, and 6 Gy. Fraction irradiations were performed as 2 Gy per time for three times with 2 days interval (2 Gy × 3). Corresponding controls were sham irradiated.

Mammosphere formation assay

Sphere formation assays were performed as described previously (Phillips *et al*, 2006).

Phosphorylated H2AX staining

Gamma-H2AX assays were performed as described previously (Muslimovic *et al*, 2008; Diehn *et al*, 2009).

In vitro colony formation assay

Colony formation assays were performed immediately after irradiation by plating cells into triplicate six-wells plates as described previously (Phillips *et al*, 2006).

In situ immunofluorescence

The chips were made as we described previously (Luo *et al*, 2008) with minor revision. In brief, purified NSCCs and CSCs were stained with the mouse monoclonal antibody against human CD133 antigen coupled with R-phycoerythrin (CD133/1(AC133)-PE from Miltenyi Biotec) together with the DNA-binding dye Hoechst 33342 (Invitrogen, Carlsbad, CA, USA) for 25 min in dark at 4 °C, washed twice, and reloaded in medium at a density of 5 × 10⁵ cells ml⁻¹, respectively. After degassing the chip, 25 µl mixtures were pipetted into the reservoir that has a total volume of about 40 µl. The cell suspension was aspirated into the cell culture rooms because of the negative pressure created by gas reabsorption of the degassed polydimethylsiloxane (PDMS). After loading of the sample, the cells in the reservoir were removed and 35 µl of

medium was added and cultured normally. After 2 h incubation, cells were photographed for the first time as described below.

For immunofluorescence staining of cells at defined time points such as 12 h or 24 h, media in reservoir was removed and 20 µl medium with appropriate concentration of CD133/1(AC133)-PE (Miltenyi Biotec) was added, and then incubated in dark at 37 °C and 5% CO₂ for 1 h to ensure the adequate solution change and staining processing by convective and diffusive mass transport (diffusion time scale is about half-an-hour). After incubation, the medium with CD133/1(AC133)-PE in reservoir was removed and 35 µl fresh medium was added and incubated in dark at 37 °C and 5% CO₂ for 30 min for washing the cells. Cells were washed twice and were immediately photographed as described below.

At defined time points such as 12 h or 24 h after cell loading, each cell culture room was captured automatically by EMCCD (Andor iXon X3, Belfast, Northern Ireland) with one DIC channel and two fluorescent channels (Hoechst 33342 for nuclei, DAPI; PE for CD133, TRITC) under ×20 objective lens (Nikon Ti-E, Tokyo, Japan). Exposure time for each channel was 20 ms. On the average, it took about 3 min to record all the cell culture rooms in a chip.

Statistical analysis

All data are pooled from at least three independent experiments and the results are presented as means ± s.d. Significance between two groups were assessed using Student's *t*-test. A *P*-value of <0.05 between groups was considered significant.

RESULTS

Enrichment of the CSCs and NSCCs

Purified CSCs and NSCCs from human SW620 colon cancer and MCF-7 breast cancer cells were isolated using fluorescence-activated cell sorting (FACS). For SW620 cells, CSCs and NSCCs were enriched via CD133 cell-surface antigen marker (Figures 1A–C) as previously reported (O'Brien *et al*, 2007; Ricci-Vitiani *et al*, 2007). The enrichment of CSCs and NSCCs is efficient, as shown in Figures 1B and C. For MCF-7 cells, CSCs and NSCCs were separated using CD44 and CD24 cell-surface antigen markers (Al-Hajj *et al*, 2003) (Supplementary Figure S1A).

Functional verification of the CSCs and NSCCs

In accordance with the phenotypic definition and presence of surface antigen markers in CSCs, the CD133⁺ and CD44⁺CD24⁻ enriched CSCs are capable of forming self-renewing spheres efficiently (Figures 1D–F and Supplementary Figure S1B). In contrast, the counterpart CD133⁻ and CD44⁺CD24⁺ NSCCs only form spheres with much less efficiency (Figures 1E and F and Supplementary Figure S1B). In addition, colony formation assay confirmed that CD133⁺ CSCs were more radioresistant than corresponding CD133⁻ NSCCs (Figures 2A and B). The preferential survival of CD133⁺ CSCs after irradiation might be because of lower rates of DNA damage, as indicated by a significantly reduced induction of γ-H2AX foci, a surrogate marker of DNA double-strand breaks (Figures 2C–F). Similar results were also found in CD44⁺CD24⁻ CSCs of MCF-7 in agreement with previous reports (Phillips *et al*, 2006) (Supplementary Figure S2).

In situ visualisation of the inter-conversion between CSCs and NSCCs

To clarify kinetics of the inter-conversion between NSCCs and CSCs, purified NSCCs or CSCs were cultured in a microfluidic chip and the expressions of CD133 cell-surface antigen marker were followed for a period of time. Figure 3A shows the typical

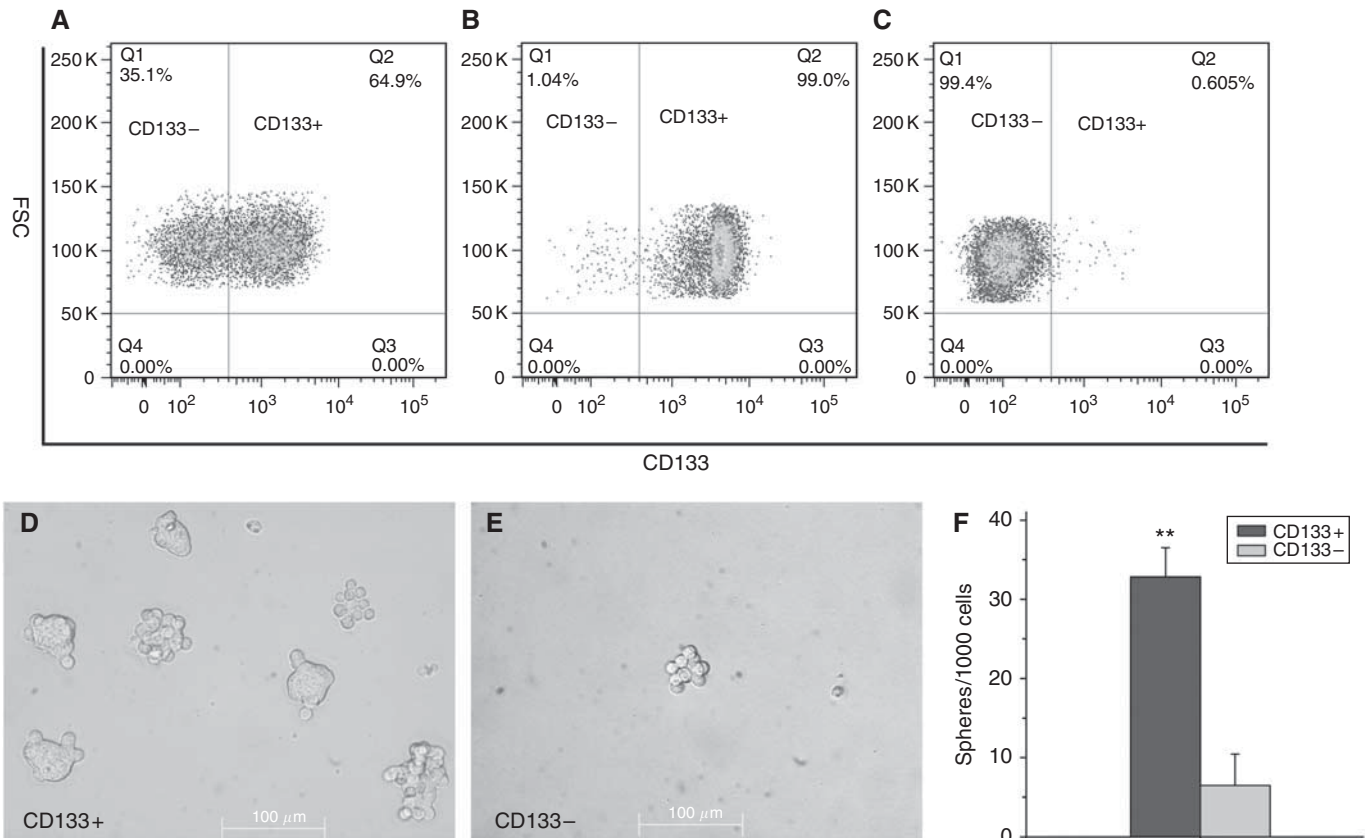


Figure 1 Enrichment of CD133⁺ CSCs and CD133⁻ NSCCs through FACS. (**A–C**) typical image of FACS sorting and efficiency. (**A**) Sorting of CD133⁺ and CD133⁻ cell subpopulation. (**B**) Typical enrichment efficiency of CD133⁺ subpopulation from **A**. (**C**) Typical enrichment efficiency of CD133⁻ subpopulation from **A**. (**D–F**) Sphere formation of CD133⁺ and CD133⁻ cells. (**D**) Typical image of sphere formations of CD133⁺ cells. (**E**) Typical image of sphere formations of CD133⁻ cells, bar=100 μ m. (**F**) Statistics in (**D** and **E**) at day 4 post inoculation (mean \pm s.d., $n=3$; ** $P=0.00109$).

platform, multi-cell culture rooms linked to a big reservoir by micro-channels of a chip. The diameter of the reservoir (illustrated by the white arrow in Figure 3A) is 4 mm, which is directly punched by a 4-mm Harris micro-puncher (Ted Pella, Redding, CA, USA). The microchannel has a dimension of 300 μ m in length, 150 μ m in width, and 35 μ m in height (as indicated with the purple arrow in Figures 3A and B). The cell culture room (indicated by the green arrow in Figures 3A and B) has a typical diameter of 400 μ m and a height of 100 μ m. The area of a single cell culture room is designed to be exactly covered by the CCD in a Live Cell Station (Nikon Ti-E). Figure 3C shows the general structure of a microfluidic chip, the substrate of the chip is made of glass, and the upper layer is PDMS with a thickness of 4 mm.

Based on *in situ* observation of >200 000 CSCs and NSCCs with the chips, it is clear that CD133⁻ NSCCs underwent spontaneous transition into CD133⁺ CSCs independent of cell division (Figures 3D–E, as indicated by arrows, white arrows for CSCs and yellow arrows for NSCCs). Furthermore, CD133⁺ CSCs could transform into CD133⁻ NSCCs but in a cell division-dependent manner. As shown in Figures 3F–I, self-renewal (one CSC symmetrically divides into two CSCs, indicated by two white arrows in Figure 3G), differentiation of CSCs into NSCCs (one CSC divides into two NSCCs, indicated by two yellow arrows in Figure 3I), and asymmetric division (one CSC asymmetrically divides into one CSC and one NSCC, indicated by one white and one yellow arrow, respectively, in Figure 3G) were observed *in situ*. Thus, under standard *in vitro* growth conditions, dedifferentiation of NSCCs to a more primitive, stem-like state (Figure 3E) and differentiation of CSCs (Figure 3I) to NSCCs occurs at the same time. The kinetics of the inter-conversion process might be very important for a better

understanding of the heterogeneity of tumour cells and might have profound impact on cancer therapy.

The inter-conversion between CSCs and NSCCs is in a homeostasis state

To further address the relationships between CSCs and NSCCs, initial cells from purified CSCs, NSCCs, and the mixture group were cultured, and the distributions of cell types were monitored by FACS over multiple generations of growth. In the purified CD133⁻ NSCCs group, CD133⁺ CSCs were detected and the proportion was found to increase with generations (Figure 4A). However, in the purified CD133⁺ CSCs group, the proportion of CD133⁻ NSCCs was also expectedly found to increase with generations. Significantly, over a period of weeks, the CSC population of purified CSCs, NSCCs, and the mixture group were stabilised at around the 65% level typical of the unsorted SW620 cell line, indicating an intrinsic homeostasis between CSCs and NSCCs (Figure 4A). The lines drawn in Figure 4 represent the best fitting of the data. Coupled with the *in situ* observational results, it is confirmed that CD133⁻ NSCCs can spontaneously generate CD133⁺ CSCs in *in vitro* cultures. Importantly, the *de novo*-created CD133⁺ subpopulations are truly CSCs, as also defined by their cell-surface markers, the ability to form spheres, and the increase in radioresistance (similar to Figure 2). We repeated the studies in MCF-7 cells and got similar results (Supplementary Figure S3A). These results demonstrate that CSCs and NSCCs in SW620 and MCF-7 cell lines are in homeostasis such that the proportion of these two cell types remains constant over many generations. The balanced inter-conversion between distinct cell

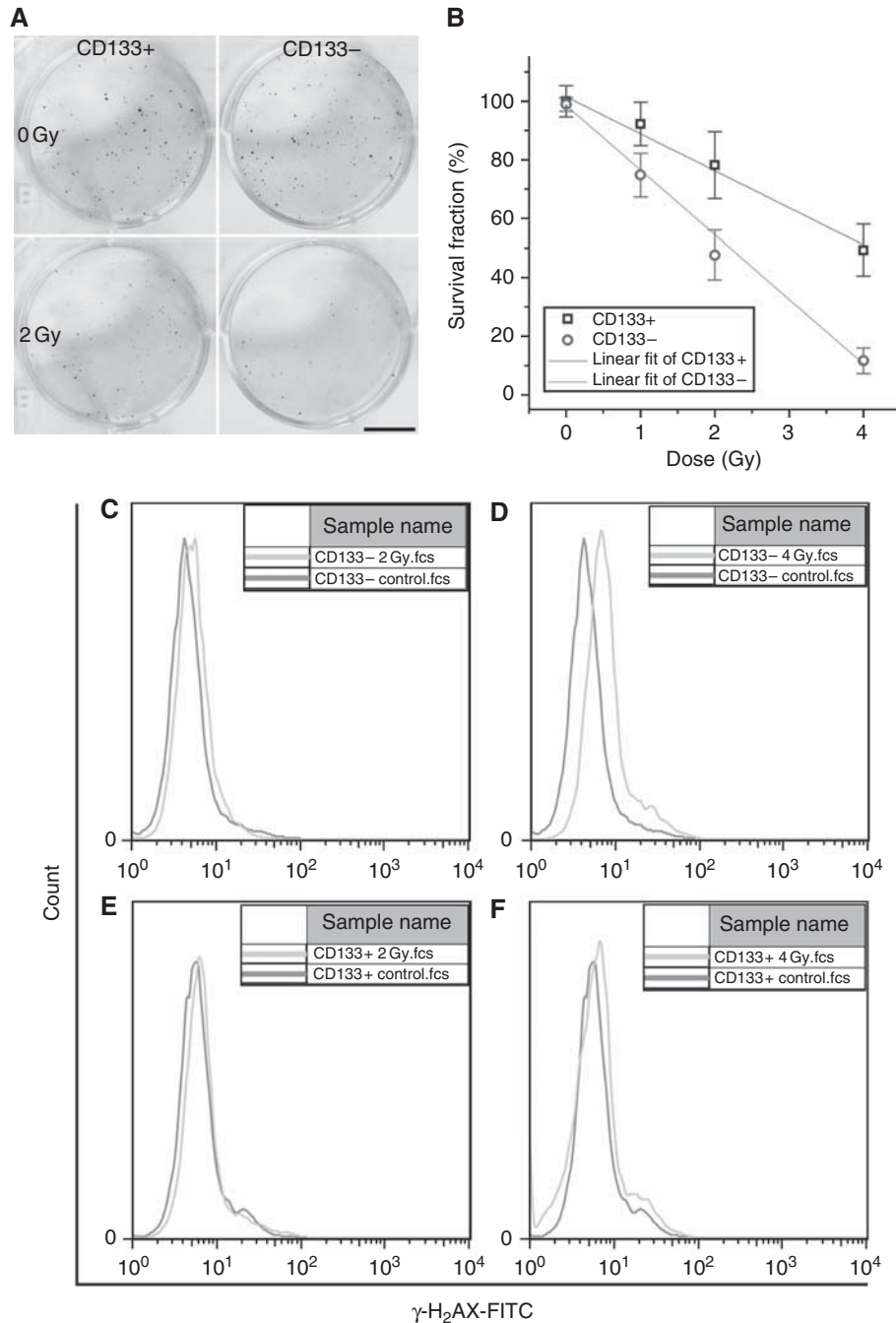


Figure 2 Radioresistance of CSCs. **(A and B)** Colony formation of CD133⁺ CSCs and CD133⁻ NSCCs with or without irradiation. **(A)** Representative colony formation images of CD133⁺ CSC and CD133⁻ NSCC controls (upper panels) and cultures irradiated with a 2-Gy dose of γ -rays (lower panels), bar = 10 mm. **(B)** Survival fractions of CD133⁺ CSCs and CD133⁻ NSCCs as a function of radiation dose. Each data point represents mean \pm s.d., $n \geq 3$. **(C-F)** γ -H₂AX assay of CD133⁺ CSCs and CD133⁻ NSCCs with or without irradiation. **(C)** Representative immunofluorescence image of γ -H₂AX analysed by flow cytometry of CD133⁻ NSCCs with or without a 2-Gy dose of γ -rays. **(D)** Similar analyses of CD133⁻ NSCCs with or without a 4-Gy dose of γ -rays. **(E)** Analyses of CD133⁺ CSCs irradiated with 2 Gy and of controls. **(F)** Analyses of CD133⁺ CSCs irradiated at 4 Gy and of controls.

types may be biologically important and relevant for maintaining the heterogeneity of cancers.

The homeostasis between CSCs and NSCCs is intrinsic and cannot be disturbed by high-dose ionising irradiation

To test the inter-conversion and the dynamic equilibrium between CSCs and NSCCs after irradiation, we exposed purified CSCs, NSCCs, and unsorted SW620 cells to γ -ray at single dose of

2 and 6 Gy and in fractions at 2 Gy \times 3. The results showed that irradiation did not disturb the final dynamic equilibrium (Figures 4B-D), although there was an initial perturbation on the homeostasis, which leads to a transient increase of CD133⁺ CSC proportion 12 h post irradiation (Figure 4E). We repeated the experiments in MCF-7 cells and got similar results (Supplementary Figure S3B). These results indicated that the homeostasis between CSCs and NSCCs is intrinsically controlled even after high dose of irradiation. This might explain the basis of local failure, which is a major therapeutic challenge after

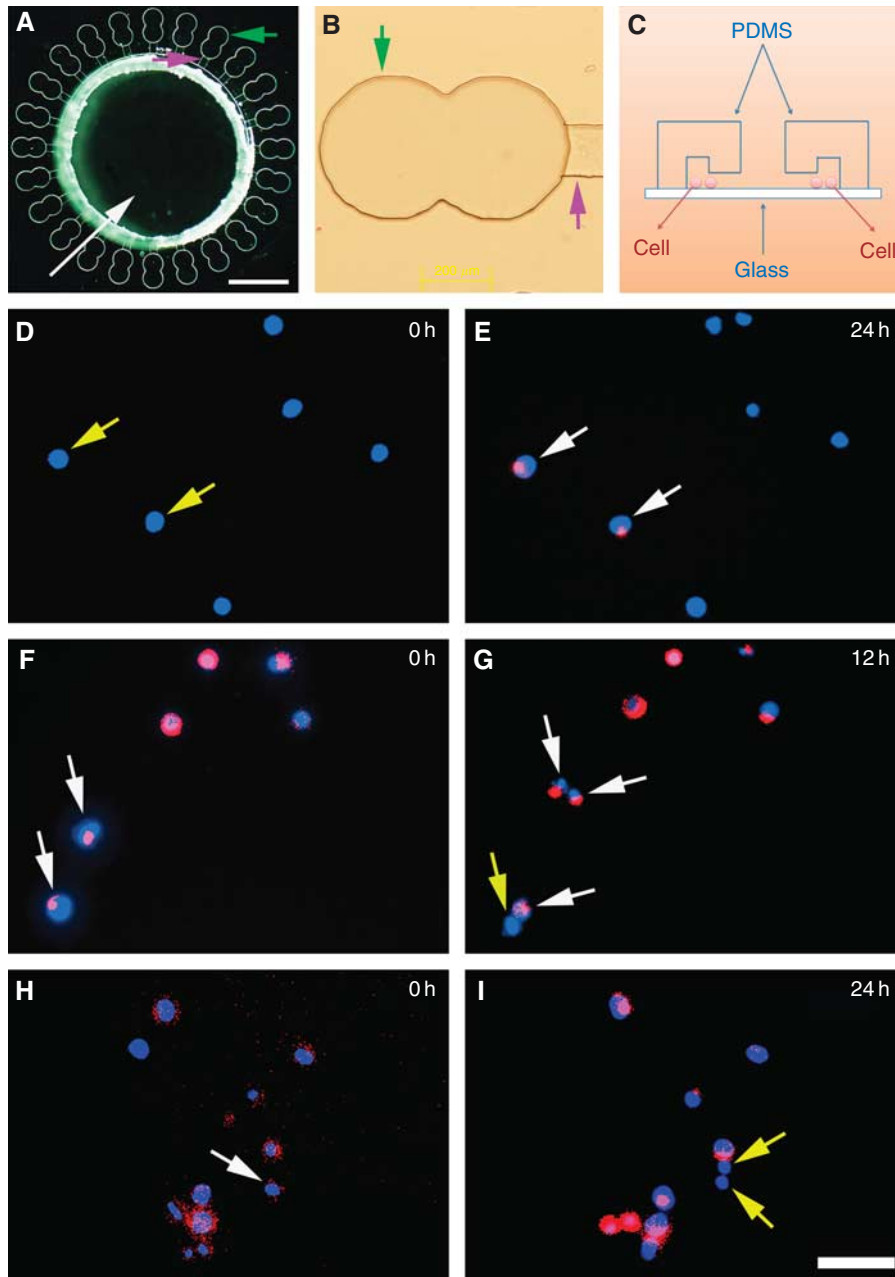


Figure 3 *In situ* immunofluorescence of CD133 expressions. (A–C) Constructed microfluidic chip for *in situ* immunofluorescence of CD133 expressions. (A) The planform of a typical chip, white arrow indicates the reservoir, green arrow indicates the cell culture room of the chip, and purple arrow indicates the micro-channel of the chip, bar = 1 mm. (B) The cell culture room (indicated as green arrow) and the channel (indicated as purple arrow) of a typical microfluidic chip, bar = 200 μm . (C) The schematic diagram of a microfluidic chip. (D and E) Typical *in situ* transition of CD133⁺ CSCs from CD133⁻ NSCCs (indicated as white arrows in E). (F and G) Typical CSC self-renewal (indicated as two white arrows in G) and asymmetric division (indicated as one white and one yellow arrow in G). (H and I) Typical differentiation of CSCs into NSCCs (indicated as two white arrow in I), bar = 50 μm for D–I. Yellow arrows indicate NSCCs and white arrows indicate CSCs. Images were merged with nuclei and CD133 expression patterns through Image-Pro Plus software (Media Cybernetics, Bethesda, MD, USA).

radiotherapy (Dalerba *et al*, 2007; Visvader and Lindeman, 2008; Clevers, 2011).

TGF- β 1-induced EMT may have important roles in the intrinsic homeostasis

The molecular mechanisms for the inter-conversion and the homeostasis remain unknown. Epithelial mesenchymal transition, a key developmental programme that is often activated during cancer metastasis and can be induced by ectopic expression

of Snail, Twist, or by exposing cells to the TGF- β 1 (Andarawewa *et al*, 2007; Thiery *et al*, 2009; Vesuna *et al*, 2009), is directly linked with *de novo* generation of CSCs. We therefore exposed the purified NSCCs cells to TGF- β 1 and quantified the dynamic proportion of CD133⁺ CSCs. The results showed that NSCCs supplemented with TGF- β 1 significantly increased the *de novo* generation of CSCs and reached the dynamic equilibrium as early as 8 days post inoculation ($P < 0.05$, Figure 5A). In contrast, treatment with SB431542, a potent and specific inhibitor of TGF- β 1 activin receptor-like kinase receptors, significantly decreased the *de novo* generation of CSCs in purified NSCCs cultures ($P < 0.05$,

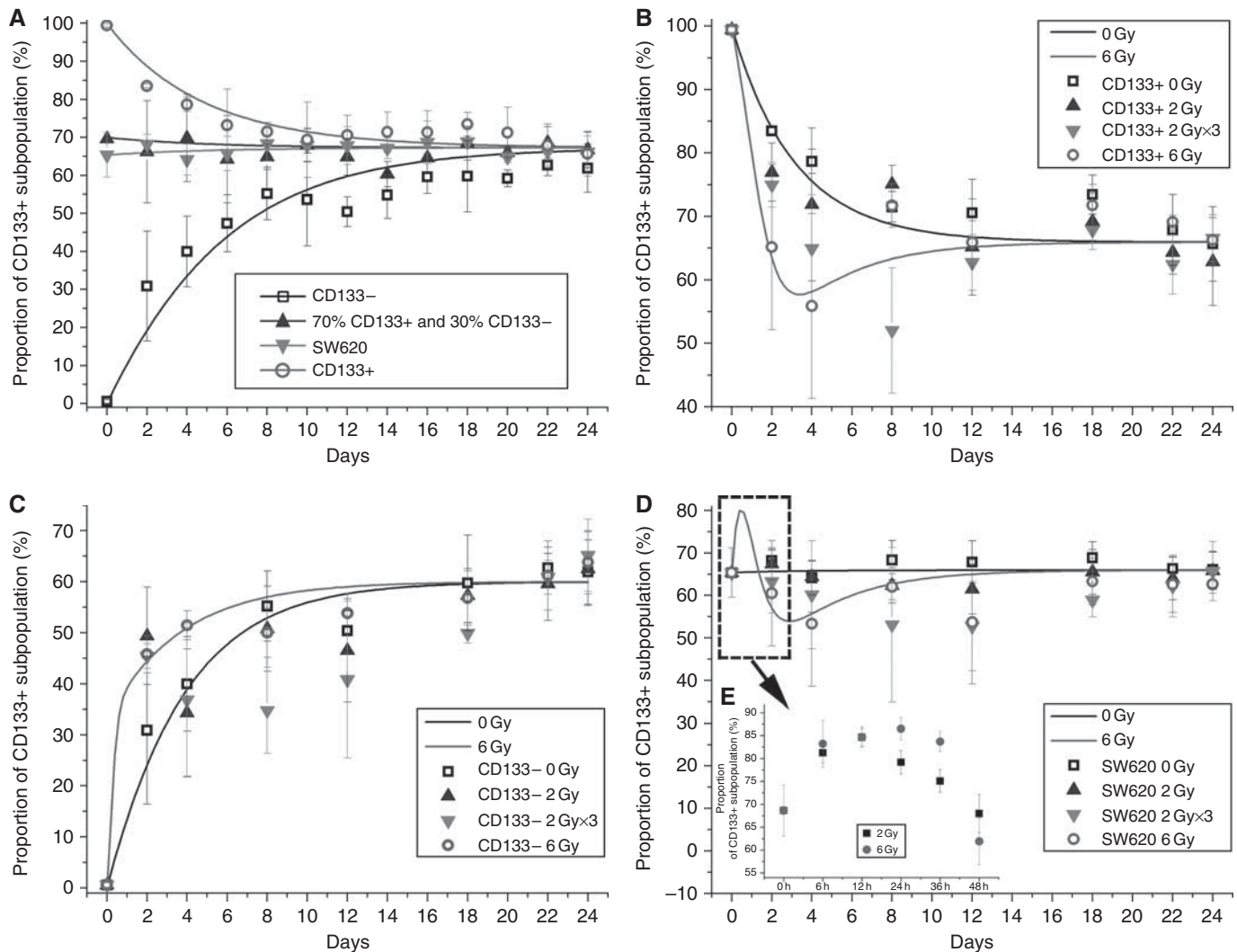


Figure 4 Intrinsic homeostasis between CD133⁺ CSCs and CD133⁻ NSCCs. **(A)** Dynamic proportion of CSC subpopulation of purified CSCs, NSCCs, mixture of the two cell types, and unsorted SW620 controls over a period of 24 days. **(B)** Dynamic proportion of CSC subpopulation in purified CD133⁺ cells with or without irradiation. **(C)** Dynamic proportion of CSC subpopulation in purified CD133⁻ NSCCs with or without irradiation. **(D)** Dynamic proportion of CSC subpopulation in unsorted SW620 cells with or without irradiation. **(E)** Details of data from the bracketed curve covering 0–48 h. Each data point represents mean \pm s.d., $n \geq 3$.

Figure 5A). In addition, treatment of unsorted SW620 cells with TGF- β 1 and SB431542 showed a slight but significant difference in the CSC proportion ($P < 0.05$, Figure 5A). Meanwhile, immunofluorescence assay of E-cadherin and Vimentin in TGF- β 1-treated NSCCs showed a significant decrease in expression of the epithelial marker E-cadherin and a significant increase in expression of the mesenchymal marker Vimentin in the conversion process (Figure 5B for E-cadherin and Figure 5C for Vimentin). These results indicated that TGF- β 1 may have important roles in the inter-conversion and the homeostasis between CSCs and NSCCs via activating the EMT process.

DISCUSSION

A key unresolved issue for cancer biology and therapy is whether the relentless growth of a tumour is driven by most of its cells or, as proposed by the CSC hypothesis, exclusively by a minor subpopulation capable of self-renewal, akin to the numerically rare normal stem cells that maintain tissues (Adams *et al*, 2007). For more effective cancer therapies, it is critical to determine which

cancer cells have the potential to contribute to the disease progression. Currently, there are two major conflicting models (Clevers, 2011). One is the traditional stochastic (clone evolution) model, which is well documented and proposes that most cancer cells can proliferate extensively and metastasise. To this view, traditional cancer therapies have sought to eliminate as many cancer cells as possible (Shackleton *et al*, 2009). The other, however, is the CSC model. The model proposes a hierarchical organisation of cells within the tumour, in which a subpopulation of stem-like cells is responsible for sustaining tumour growth (Visvader and Lindeman, 2008). To this view, anti-tumour treatments are specifically designed to target CSCs, although theoretically unable to cause rapid shrinkage of tumour lesions, it might nonetheless achieve long-term disease eradication by exhausting self-renewal and growth potential of cancer tissues (Dalerba *et al*, 2007). Our results clarified the inter-conversion *in situ* between CSCs and NSCCs (Figure 3). In addition, the inter-conversion between CSCs and NSCCs is also found in a homeostasis state (Figure 4A). To maintain a stable equilibrium, the rates of CSC differentiation, self-renewal, and asymmetric division should be balanced by the rate of transitions of CSCs from

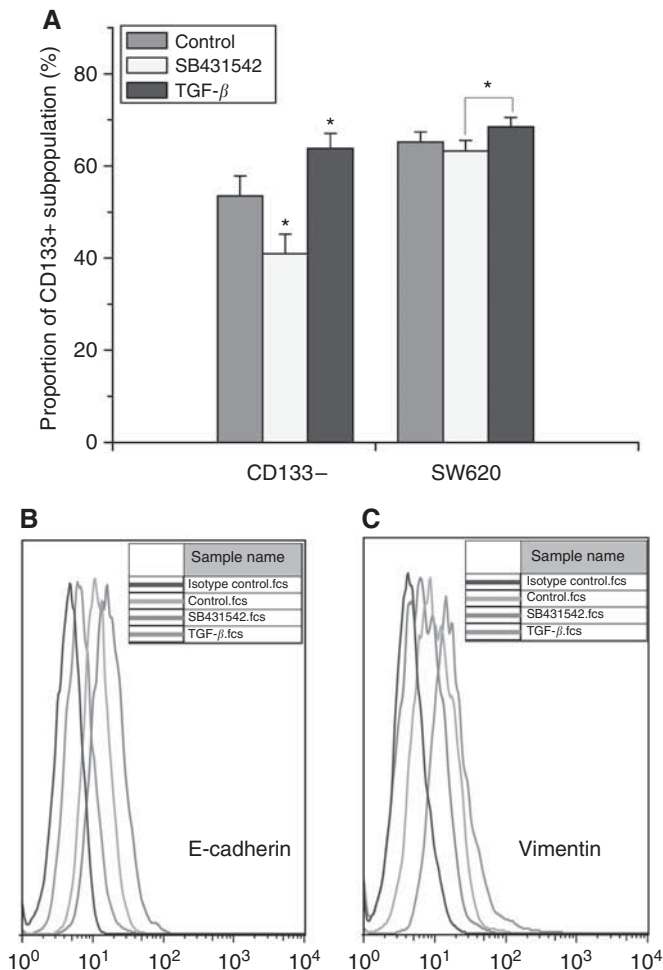


Figure 5 TGF- β 1 might have important roles in the inter-conversion and homeostasis between NSCCs and CSCs via activating EMT. **(A)** Exogenous supplement of TGF- β 1 accelerates transition of CSCs from NSCCs (mean \pm s.d., $n = 3$; $*P = 0.02982$), whereas SB431542 inhibits the transition (mean \pm s.d., $n = 3$; $*P = 0.02395$); TGF- β 1- and SB431542-treated unsorted SW620 cells showed a significant difference in CSC proportion (mean \pm s.d., $n = 3$; $*P = 0.03757$). **(B)** Expressions of E-cadherin in purified NSCCs with or without TGF- β 1 and SB431542. **(C)** Expressions of Vimentin in purified NSCCs with or without TGF- β 1 and SB431542. Data was detected through FACS at day 8 post inoculation.

NSCCs, which might depend on the proportion of CSCs in the population. These results, together with several other recent studies (Mani *et al*, 2008; Morel *et al*, 2008; Meyer *et al*, 2009; Liang *et al*, 2010; Chaffer *et al*, 2011; Iliopoulos *et al*, 2011), indicate that some cancer cells retain the capacity to convert to a more primitive, stem-like state when adapting to changing conditions, indicating a need to reconcile the current stochastic and CSC models of tumour progression (Alison *et al*, 2011; Clevers, 2011).

The microfluidic chip used in present study was designed to overcome several difficulties commonly encountered under *in situ* cell observations. First, positioning and relocating of target cells on a micrometre scale are the basis of *in situ* observation. Cells cultured in normal dish or chamber slide cannot achieve the high precision goal. Second, cells cultured in dishes or chamber slide are easily movable when changing the medium. In *in situ* observations, immunostaining, washing, and reloading of the medium will lead to significant movement of the cells being followed. Third, shear force needs to be minimised in all of the

procedures to ensure little mechanical damage to cells. With the designed chips and a Live Cell Station, we clarified the inter-conversion between CSCs and NSCCs *in situ* (Figure 3).

Ionising radiation is a widely used treatment modality for various solid tumours and about 60% of cancer patients receive radiation therapy (Garcia-Barros *et al*, 2003). The CSC hypothesis suggests that standard radiotherapy can effectively kill NSCCs but CSCs largely survive because of the intrinsic radioresistance and thereafter reinitiate the bulk of the tumour (Dalerba *et al*, 2007; Cui *et al*, 2011; Iliopoulos *et al*, 2011). Our experimental results show that the dynamic equilibrium in a given cell group might be intrinsic and might be resistant to disturbance by external factors such as high-dose irradiation (Figures 4B–D). Logically, due to the radioresistant nature of CSCs, CSC proportion in tumour is expected to be transiently higher after irradiations (Figure 4E). However, given the equilibrium for homeostasis control of the cell subpopulations, it is possible that higher CSC proportion might increase their differentiation into NSCCs to repopulate tumour cells. This may indicate a possible mechanism of local failure, which is one of the major therapeutic challenges after radiotherapy (Visvader and Lindeman, 2008).

The molecular mechanisms for the inter-conversion and the homeostasis between CSCs and NSCCs largely remain unknown. It is well known that co-expression of pluripotency markers, such as Oct3/4, Sox2, c-myc, Klf4, Nanog and lin28, can reprogram somatic cells into pluripotent embryonic stem-like cells (Takahashi and Yamanaka, 2006; Yu *et al*, 2007). Likewise, studies also showed that single or combined overexpression of stemness factors, including Oct-4 and Nanog, were associated with cancer stem-like properties and EMT induction (Chiou *et al*, 2010; Chen *et al*, 2012; Kumar *et al*, 2012). Epithelial mesenchymal transition, a key developmental programme that is often activated during cancer metastasis and can be induced by ectopic expression of Oct-4 (Chiou *et al*, 2010), Twist (Vesuna *et al*, 2009), by inhibition of proteasome (Kim *et al*, 2011), or even by treatment with irradiation and/or TGF- β (Andarawewa *et al*, 2007), is directly linked with *de novo* generation of CSCs (Mani *et al*, 2008; Thiery *et al*, 2009). As inhibition of proteasome can cause EMT and generate cells with stem-like properties (Kim *et al*, 2011), the low proteasome activities might be also involved in the *de novo* generations of CD133⁺ CSCs from CD133⁻ NSCCs. In addition, irradiation can activate EMT and evoke a rapid inhibitory effect on proteasome function in a variety of cell types (Pajonk and McBride, 2001; Andarawewa *et al*, 2007), therefore, despite of the radioresistance nature of CSCs, transient induction of CD133 accumulation via EMT activation and/or proteasome inhibition might be also involved in the transient increase of CD133⁺ cells after irradiations (Figure 4E). Our results showed that irradiation and TGF- β treatment can accelerate the inter-conversion and homeostasis between CSCs and NSCCs (Figures 4C and 5A), together with significant decrease in expression of the epithelial marker E-cadherin and significant increase in expression of the mesenchymal marker Vimentin in the conversion (Figures 5B–C), suggesting EMT might have important roles in the inter-conversion and homeostasis between CSCs and NSCCs.

ACKNOWLEDGEMENTS

We thank Jiuqiang Li and Deliang Sun for the help of irradiation and Lili Ji and Chunchun Liu for the help of FACS assay. This work was supported by grants from the US National Institutes of Health (5P0-CA 49062-19), the Key Project of National Natural Science Foundation of China (10935009), and the National Science Foundation for Young Scholars of China (31000383).

Supplementary Information accompanies the paper on British Journal of Cancer website (<http://www.nature.com/bjc>)

REFERENCES

- Achuthan S, Santhoshkumar TR, Prabhakar J, Nair SA, Pillai MR (2011) Drug-induced senescence generates chemoresistant stemlike cells with low reactive oxygen species. *J Biol Chem* **286**(43): 37813–37829
- Adams JM, Kelly PN, Dakic A, Nutt SL, Strasser A (2007) Response to comment on 'tumor growth need not be driven by rare cancer stem cells'. *Science* **318**(5857): 1722
- Al-Hajj M, Wicha MS, Benito-Hernandez A, Morrison SJ, Clarke MF (2003) Prospective identification of tumorigenic breast cancer cells. *Proc Natl Acad Sci USA* **100**(7): 3983–3988
- Alison MR, Lim SML, Nicholson LJ (2011) Cancer stem cells: problems for therapy? *J Pathol* **223**(2): 148–162
- Andarawewa KL, Erickson AC, Chou WS, Costes SV, Gascard P, Mott JD, Bissell MJ, Barcellos-Hoff MH (2007) Ionizing radiation predisposes nonmalignant human mammary epithelial cells to undergo transforming growth factor beta induced epithelial to mesenchymal transition. *Cancer Res* **67**(18): 8662–8670
- Bao S, Wu Q, McLendon RE, Hao Y, Shi Q, Hjelmeland AB, Dewhirst MW, Bigner DD, Rich JN (2006) Glioma stem cells promote radioresistance by preferential activation of the DNA damage response. *Nature* **444**(7120): 756–760
- Chaffer CL, Brueckmann I, Scheel C, Kaestli AJ, Wiggins PA, Rodrigues LO, Brooks M, Reinhardt F, Su Y, Polyak K, Arendt LM, Kuperwasser C, Biebric M, Weinberg RA (2011) Normal and neoplastic nonstem cells can spontaneously convert to a stem-like state. *Proc Natl Acad Sci USA* **108**(19): 7950–7955
- Chen Z, Wang T, Cai L, Su C, Zhong B, Lei Y, Xiang AP (2012) Clinicopathological significance of non-small cell lung cancer with high prevalence of Oct-4 tumor cells. *J Exp Clin Cancer Res* **31**(1): 10
- Chiou SH, Wang ML, Chou YT, Chen CJ, Hong CF, Hsieh WJ, Chang HT, Chen YS, Lin TW, Hsu HS, Wu CW (2010) Coexpression of Oct4 and Nanog enhances malignancy in lung adenocarcinoma by inducing cancer stem cell-like properties and epithelial-mesenchymal trans differentiation. *Cancer Res* **70**(24): 10433–10444
- Clevers H (2011) The cancer stem cell: premises, promises and challenges. *Nat Med* **17**(3): 313–319
- Cui X, Oonishi K, Tsujii H, Yasuda T, Matsumoto Y, Furusawa Y, Akashi M, Kamada T, Okayasu R (2011) Effects of carbon ion beam on putative colon cancer stem cells and its comparison with X-rays. *Cancer Res* **71**(10): 3676–3687
- Dalerba P, Cho RW, Clarke MF (2007) Cancer stem cells: models and concepts. *Annu Rev Med* **58**: 267–284
- Diehn M, Cho RW, Lobo NA, Kalisky T, Dorie MJ, Kulp AN, Qian D, Lam JS, Ailles LE, Wong M, Joshua B, Kaplan MJ, Wapnir I, Dirbas FM, Somlo G, Garberoglio C, Paz B, Shen J, Lau SK, Quake SR, Brown JM, Weissman IL, Clarke MF (2009) Association of reactive oxygen species levels and radioresistance in cancer stem cells. *Nature* **458**(7239): 780–783
- Garcia-Barros M, Paris F, Cordon-Cardo C, Lyden D, Rafii S, Haimovitz-Friedman A, Fuks Z, Kolesnick R (2003) Tumor response to radiotherapy regulated by endothelial cell apoptosis. *Science* **300**(5622): 1155–1159
- Iliopoulos D, Hirsch HA, Wang G, Struhl K (2011) Inducible formation of breast cancer stem cells and their dynamic equilibrium with non-stem cancer cells via IL6 secretion. *Proc Natl Acad Sci USA* **108**(4): 1397–1402
- Kim JY, Nam JK, Lee SA, Lee MS, Cho SK, Park ZY, Lee JW, Cho M (2011) Proteasome inhibition causes epithelial-mesenchymal transition upon TM4SF5 expression. *J Cell Biochem* **112**(3): 782–792
- Kumar SM, Liu S, Lu H, Zhang H, Zhang PJ, Gimotty PA, Guerra M, Guo W, Xu X (2012) Acquired cancer stem cell phenotypes through Oct4-mediated dedifferentiation. *Oncogene*; e-pub ahead of print 30 January 2012; doi:10.1038/onc.2011.656
- Liang Y, Zhong Z, Huang Y, Deng W, Cao J, Tsao G, Liu Q, Pei D, Kang T, Zeng YX (2010) Stem-like cancer cells are inducible by increasing genomic instability in cancer cells. *J Biol Chem* **285**(7): 4931–4940
- Luo C, Zhu X, Yu T, Luo X, Ouyang Q, Ji H, Chen Y (2008) A fast cell loading and high-throughput microfluidic system for long-term cell culture in zero-flow environments. *Biotechnol Bioeng* **101**(1): 190–195
- Mani SA, Guo W, Liao MJ, Eaton EN, Ayyanan A, Zhou AY, Brooks M, Reinhard F, Zhang CC, Shipitsin M, Campbell LL, Polyak K, Brisken C, Yang J, Weinberg RA (2008) The epithelial-mesenchymal transition generates cells with properties of stem cells. *Cell* **133**(4): 704–715
- Meyer MJ, Fleming JM, Ali MA, Pesesky MW, Ginsburg E, Vonderhaar BK (2009) Dynamic regulation of CD24 and the invasive, CD44posCD24neg phenotype in breast cancer cell lines. *Breast Cancer Res* **11**(6): R82
- Morel AP, Lievre M, Thomas C, Hinkal G, Ansieau S, Puisieux A (2008) Generation of breast cancer stem cells through epithelial-mesenchymal transition. *PLoS One* **3**(8): e2888
- Muslimovic A, Ismail IH, Gao Y, Hammarsten O (2008) An optimized method for measurement of gamma-H2AX in blood mononuclear and cultured cells. *Nat Protoc* **3**(7): 1187–1193
- O'Brien CA, Pollett A, Gallinger S, Dick JE (2007) A human colon cancer cell capable of initiating tumour growth in immunodeficient mice. *Nature* **445**(7123): 106–110
- Pajonk F, McBride WH (2001) Ionizing radiation affects 26s proteasome function and associated molecular responses, even at low doses. *Radiother Oncol* **59**(2): 203–212
- Phillips TM, McBride WH, Pajonk F (2006) The response of CD24(−/low)/CD44+ breast cancer-initiating cells to radiation. *J Natl Cancer Inst* **98**(24): 1777–1785
- Ricci-Vitiani L, Lombardi DG, Pilozzi E, Biffoni M, Todaro M, Peschle C, De Maria R (2007) Identification and expansion of human colon-cancer-initiating cells. *Nature* **445**(7123): 111–115
- Rosen JM, Jordan CT (2009) The Increasing Complexity of the Cancer Stem Cell Paradigm. *Science* **324**(5935): 1670–1673
- Shackleton M, Quintana E, Fearon ER, Morrison SJ (2009) Heterogeneity in cancer: cancer stem cells versus clonal evolution. *Cell* **138**(5): 822–829
- Takahashi K, Yamanaka S (2006) Induction of pluripotent stem cells from mouse embryonic and adult fibroblast cultures by defined factors. *Cell* **126**(4): 663–676
- Thiery JP, Acloque H, Huang RY, Nieto MA (2009) Epithelial-mesenchymal transitions in development and disease. *Cell* **139**(5): 871–890
- Vesuna F, Lisok A, Kimble B, Raman V (2009) Twist modulates breast cancer stem cells by transcriptional regulation of CD24 expression. *Neoplasia* **11**(12): 1318–1328
- Visvader JE, Lindeman GJ (2008) Cancer stem cells in solid tumours: accumulating evidence and unresolved questions. *Nat Rev Cancer* **8**(10): 755–768
- Quan Y, Wang W, Fu Q, Mei T, Wu J, Li J, Yang G, Wang Y (2011) Accumulation efficiency of cancer stem-like cells post γ -ray and proton irradiation. *Nucl Instr Meth B*; e-pub ahead of print 22 November 2011; doi:10.1016/j.nimb.2011.11.019
- Yu J, Vodyanik MA, Smuga-Otto K, Antosiewicz-Bourget J, Frane JL, Tian S, Nie J, Jonsdottir GA, Ruotti V, Stewart R, Slukvin II, Thomson JA (2007) Induced pluripotent stem cell lines derived from human somatic cells. *Science* **318**(5858): 1917–1920

This work is published under the standard license to publish agreement. After 12 months the work will become freely available and the license terms will switch to a Creative Commons Attribution-NonCommercial-Share Alike 3.0 Unported License.